Macromolecules
Cite This: Macromolecules 2018, 51, 6334−6343
Article
pubs.acs.org/Macromolecules

Diffusion Behavior of Methanol Molecules Confined in Cross-Linked Phenolic Resins Studied Using Neutron Scattering and Molecular Dynamics Simulations

Yasuyuki Shudo,*[,†,‡] Atsushi Izumi,[‡] Katsumi Hagita,[§] Takeshi Yamada,[∥] Kaoru Shibata,[⊥] and Mitsuhiro Shibayama*[,†]

[†]Neutron Science Laboratory, Institute for Solid State Physics, The University of Tokyo, 5-1-5 Kashiwanoha, Kashiwa, Chiba 277-8581, Japan

[‡]Corporate Engineering Center, Sumitomo Bakelite Co., Ltd., 2100, Takayanagi, Fujieda, Shizuoka 426-0041, Japan

[§]Department of Applied Physics, National Defense Academy, 1-10-20, Hashirimizu, Yokosuka, Kanagawa 239-8686, Japan

[∥]Neutron Science and Technology Center, Comprehensive Research Organization for Science and Society, 162-1 Shirakata, Tokai, Naka, Ibaraki 319-1106, Japan

[⊥]Materials and Life Science Division, J-PARC Center, Japan Atomic Energy Agency, 2-4 Shirakata, Tokai, Naka, Ibaraki 319-1195, Japan

Supporting Information

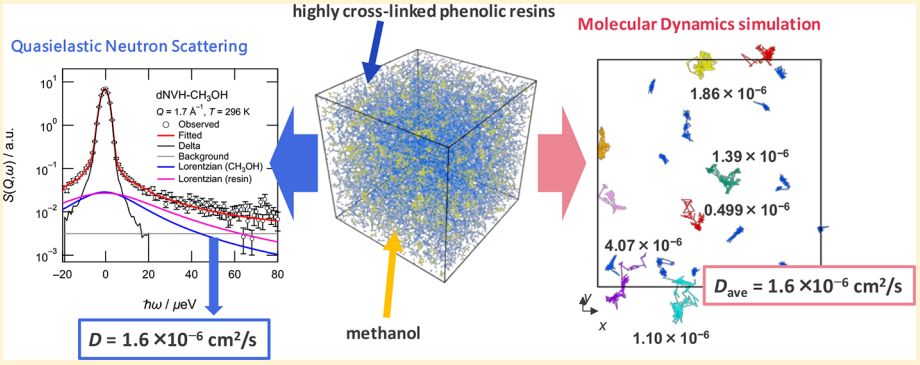

ABSTRACT: The dynamics of methanol confined in highly cross-linked phenolic resins was investigated using incoherent quasielastic neutron scattering (QENS) and atomistic molecular dynamics (MD) simulations. The QENS analysis for a deuterated phenolic resin and both deuterated and nondeuterated methanol indicated the presence of resin dynamics induced by methanol invasion and confined diffusion of the methanol molecules. QENS results suggested that methanol had a diffusion coefficient of 1.6×10^{-6} cm^2/s, which is 1 order of magnitude smaller than the bulk value (2.3×10^{-5} cm^2/s). The MD trajectories also showed that the methanol diffusion was limited by the resin network, consistent with QENS results in terms of the diffusion coefficient and diffusion-like behavior.

1. INTRODUCTION

Highly cross-linked thermosetting resins, such as phenolic resins and epoxy resins, exhibit excellent properties, such as strong mechanical properties, thermal stability, electric resistance, and solvent resistance, owing to their dense chemically bonded network structures.[1−3] These materials are widely used in many industrial applications, such as in automobiles, semiconductors, and aerospace equipment. For automotive parts and semiconductor packages, high solvent resistance is required because such materials may be exposed to various solvents under prolonged conditions of high temperature and pressure. Solvent penetration into cured thermosetting resins causes many problems, including dimensional changes, decreases in mechanical strength and modulus (leading to solvent stress cracking), and short-circuiting. In designing thermosetting materials, it is necessary to understand the relationships between a cross-linked structure and solvent resistance. Elucidation of the diffusion mechanism of small molecules, such as water, methanol, or ethanol, in cured resins is of special importance for achieving high solvent resistance.

The diffusion coefficient (D) of the penetrating solvent molecule is considered an important parameter for characterizing solvent resistance. In general, measurements of weight change for a piece of test material are often used to estimate the diffusion coefficient.[3] Kaplan et al. investigated the solvent penetration behavior in cured epoxy resins to elucidate the

Received: March 12, 2018
Revised: July 23, 2018
Published: August 10, 2018

DOI: 10.1021/acs.macromol.8b00535
Macromolecules 2018, 51, 6334−6343

influence of various penetrant solvents, cross-linking agents, and temperature.[4] They assumed a simple Fickian diffusion model for solvent transport. The differential equation of Fick's second law in the one-dimensional case was given for weight change as a function of D and time. D was estimated by the weight change curve. Soles et al. investigated the effect of nanovoid size, molecular flexibility, and temperature on the moisture diffusion coefficient for typical epoxy resins using similar diffusion measurements together with positron annihilation lifetime spectroscopy (PALS).[5] They proposed a molecular mechanism for moisture transport in epoxy resins from the transport kinetics, in which water molecules in the cured epoxy network form hydrogen bonds with the polar group of the epoxy resins (hydroxyl or amine groups) and diffuse in the nanovoid space. Here, the dominant factor for the moisture diffusion coefficient was the lifetime of hydrogen bonding, not the size or shape of the nanovoid spaces in the network.[6]

One of the problems of adsorption experiments is that it takes several days to several months to obtain a solvent uptake curve. Furthermore, it is necessary to prepare an ideal plate-shaped test piece with a flat and smooth surface. The most critical problem of this method is that it cannot be applied to the case of non-Fickian diffusion behavior. As seen in Kaplan's experiments, no clear equilibrium point may be seen in the weight-change curve, which indicates the presence of irreversible processes.

Quasielastic neutron scattering (QENS) is a powerful technique for investigating the dynamics of molecular diffusion in liquids or the fast relaxation processes in polymer chains.[7−9] QENS is able to detect molecular motion over a time scale of 1 ps to 10 ns with a spatial scale of 1−100 Å. This space−time scale corresponds to molecular vibrations, rotations, and translations. Accordingly, QENS analysis provides atomistic-order information on the molecular structure and the molecular dynamics. Although the diffusion coefficient (D) of molecules can also be characterized by other methods, like pulse field gradient nuclear magnetic resonance (PFG-NMR) spectroscopy, most methods do not provide information on the atomistic spatial scale.[10] Furthermore, the space−time scale of QENS is almost consistent with that of an atomistic molecular dynamics (MD) simulation. Many studies have proved that combination analysis using QENS and MD simulations is a very powerful technique for providing a basic understanding of molecular motion.[11,12]

In incoherent QENS, the scattering intensity originates from the incoherent scattering cross sections (σ_{inc}). The value of σ_{inc} in hydrogen is 80.27 barn, which is much larger than that of deuterium (2.05 barn). Therefore, for most organic materials, the dynamics of a target component (including hydrogen) can be efficiently detected by deuteration of the other components. There are many incoherent QENS studies on the self-diffusion behavior of bulk liquids and polymers. Bermejo investigated the diffusion behavior of bulk methanol by QENS in detail,[13] and the estimated value of D in translational diffusion correlated well with the value measured using other techniques, such as PFG-NMR.[14] The dynamics of small molecules in confined spaces was also investigated by many researchers using QENS. Takahara et al. investigated the dynamics of water, methanol, and ethanol confined in porous silica using QENS and dielectric analyses.[15−17] The constrained dynamics of small molecules confined in zeolites,[18] carbon nanotubes,[19] and micelles[20] have also been investigated using QENS. These studies reported that the D of small molecules in confined spaces was 1 order of magnitude smaller compared with those in the bulk state.

In contrast to these studies, QENS studies on the dynamics of liquids confined in cured thermosetting resins have not been reported so far. One reason for this lack of study is that thermosetting resins contain a large amount of hydrogen atoms and lead to larger incoherent scattering than that of penetrated solvent, as mentioned above. In general, deuteration of most thermosetting resins is not trivial because of synthetic difficulties and costs. Therefore, QENS has not been applied for cured thermosetting polymers, except by Rosenberg, Jørgensen, and Arai for fracton dimension analysis of cured epoxy resins.[21−23] For phenolic resins, we succeeded in synthesizing highly deuterated novolac resins (dNV) through polycondensation of phenol-d_6 and formaldehyde-d_2.[24] The results of the ^{1}H NMR analysis for dNV showed that the degree of deuteration, except for the hydroxyl group, was >98%, and the small-angle neutron scattering (SANS) intensity for the cured resin with hexamethylenetetramine (HMTA) exhibited a much lower incoherent scattering background than that of the nondeuterated phenolic resin. Subsequently, we performed small-angle X-ray scattering (SAXS) and SANS experiments for dNV and cured dNV to investigate the structural inhomogeneities in the cross-linking networks.[25] This complementary analysis indicated the presence of nanovoids in the cured resins. The scattering intensity in the range from 3 to 1600 nm was mainly accounted for by the internal fractal interfaces between nanovoids and resins. These results suggested that penetrated solvent molecules existed in the resin nanovoids.

Molecular dynamics (MD) simulations for small molecule diffusion have been reported for many systems, such as for bulk liquids and small molecules in confined spaces. In an MD simulation, D can be estimated by calculating the mean squared displacement of each molecule or the velocity autocorrelation function from the MD trajectories.[26,27] Solvent diffusion in cured polymer networks is a subject of interest in MD simulations of thermosetting resins. Yarovsky et al. reported the modeling of cured networks for phosphate modified epoxy resins and cross-linkers and the diffusion of water and oxygen in cured networks.[28] Wu et al. investigated moisture content dependence on the structure and D of water in cured bisphenol A type epoxy resin.[29] It is well-known that, in the simulation of thermosetting resins, the modeling method of the cross-linked structure greatly affects the calculation results.[30] Therefore, the structure used in an MD simulation has to be thoroughly examined beforehand. We performed atomistic MD simulations on a phenolic resin model constructed using pseudo-cross-link reactions[31,32] and mechanical property characterizations.[33] The obtained model structure was verified by comparison with experimental data on the chemical structure and X-ray scattering profiles. We confirmed that a large-scale atomistic MD simulation with optimized reaction parameters was appropriate for representing the cross-linked structure, including the cross-link inhomogeneity observed by SAXS experiments using the solvent swelling technique.[34−36] This model structure can be used as an initial structure to calculate solvent diffusion in a cross-linked phenolic network.

In this paper, we report the diffusion dynamics of methanol confined in highly cross-linked phenolic resins, as investigated using QENS and atomistic MD simulations. Methanol was

DOI: 10.1021/acs.macromol.8b00535
Macromolecules 2018, 51, 6334−6343

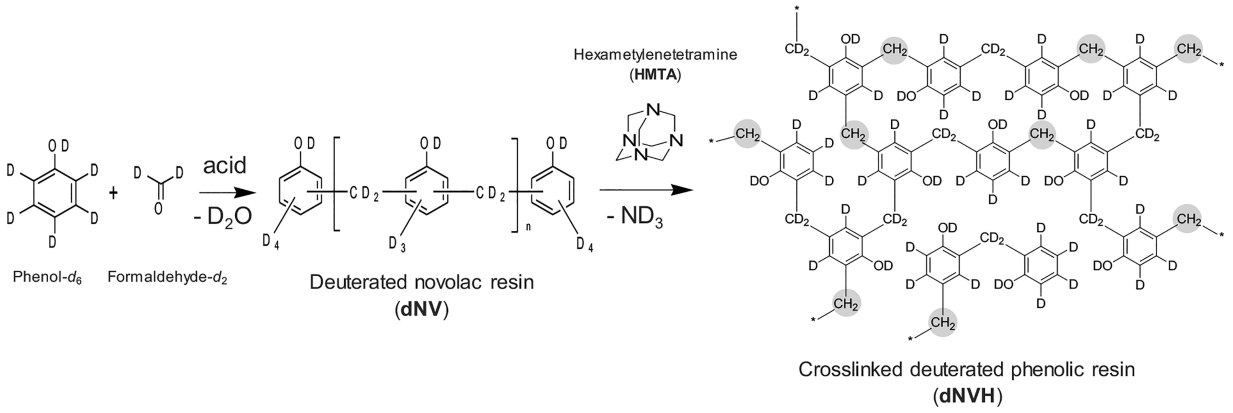

Figure 1. Synthesis of highly deuterated phenolic resin (dNV) and cross-linked resin (dNVH).

chosen as the penetrating solvent because methanol is empirically known to be a solvent that is easily absorbed in cured phenolic resins. A highly deuterated phenolic resin cured with HMTA was used after immersion in methanol or deuterated methanol for the QENS experiments. The incoherent scattering from the methanol molecules was selectively analyzed by model fitting with a Lorentz function using the difference in incoherent scattering cross sections of hydrogen and deuterium. The diffusion behavior of methanol was discussed on the basis of the diffusion model in confined space. Atomistic MD simulations were also performed on the methanol-dispersed cross-linked phenolic resin model. The diffusion coefficient calculated from the MD trajectories was compared with the QENS result.

2. METHOD

2.1. Materials. For QENS experiments, highly deuterated cross-linked phenolic resins were prepared via two processes: synthesis of deuterated novolac resin (i.e., phenolic resin oligomer) and subsequent cross-link reaction using a curing agent, as shown in Figure 1. Phenol-d_6 (98.9 atom % D) and 20 wt % formaldehyde-d_2 (99.8 atom % D) in D_2O were purchased from C/D/N isotopes Inc. Oxalic acid and hexamethylenetetramine (HMTA) were purchased from Wako Pure Chemical Industries and Chang Chun Petrochemical Co., Ltd., respectively. Methanol-d_4 (CD_3OD, 99.8 atom % D) and methanol (CH_3OH) were purchased from Cambridge Isotope Laboratories, Inc., and Wako Pure Chemical Industries, respectively. All materials were used without further purification. Deuterated novolac-type phenolic resin (dNV) was synthesized from phenol-d_6 and 20 wt % formaldehyde-d_2 in D_2O according to our previous study.[24]

2.2. Sample Preparation for QENS Experiments. A plate-like test piece of cured phenolic resin (dNVH) was prepared from dNV and HMTA as a curing agent by compression molding using a compression molding machine (Shinto Metal Industries Corp., Osaka, Japan). Granulated dNV and HMTA were placed in a molding die and molded at 175 °C for 3 min under an effective pressure of 100 MPa, followed by postcuring at 180 °C for 6 h and 220 °C for 3 h under atmospheric pressure. The approximate size of the test pieces was 10 mm × 80 mm with 2 mm thickness. The sample (dNVH) and solvent (CH_3OH or CD_3OD) were sealed in a pressure vessel and allowed to stand for 72 h in an 80 °C oven. Then, the sample was dried in the air and pulverized with a mill for QENS measurement. The powdered sample was abbreviated as dNVH−CH_3OH and dNVH−CD_3OD. The dried dNVH was also prepared for the comparison. The amount of penetrant methanol in dNVH−CH_3OH and dNVH−CD_3OD was estimated to be about 8 wt % from the weight change measurement value after heating in a vacuum oven at 120 °C for 1 h.

From the composition of dNVH and methanol in dNVH−CH_3OH, the calculated number ratio of H atoms and D atoms is given as H_{dNVH}:D_{dNVH}:H_{CH3OH} = 1:5.6:1.6. Accordingly, the ratio of incoherent scattering cross sections (σ_{inc}) is given as $\sigma_{inc}(H_{dNVH})$:$\sigma_{inc}(D_{dNVH})$:$\sigma_{inc}(H_{CH3OH})$ = 6.9:1:11.1. This suggests that sufficient incoherent scattering intensity from the CH_3OH in the dNVH−CH_3OH can be obtained by the QENS measurement for dNVH−CH_3OH. However, 42% in the incoherent scattering intensity in the dNVH−CH_3OH originates mainly from the methylene groups in the dNVH. In contrast, the incoherent scattering intensity of the methylene groups in dNVH−CD_3OD is dominant (96% in the incoherent scattering). Comparing between dNVH−CH_3OH and dNVH−CD_3OD, the incoherent scattering from the CH_3OH can be extracted.

2.3. Quasielastic Neutron Scattering (QENS) Measurements. QENS experiments were performed using the time-of-flight near-backscattering spectrometer (DNA, BL02) installed at the Materials and Life Science Experimental Facility (MLF) of J-PARC, located in Tokai, Ibaraki, Japan.[37−39] Powder samples were lapped with thin aluminum foil (40 mm height, 44 mm width) and were loaded in a cylindrical aluminum sample holder (14.0 mm in inner diameter of the cylinder with 0.25 mm thickness) in a high-purity helium-gas atmosphere. The sample holder was sealed using an indium gasket. The dynamic scattering functions $S(Q, \omega)$ were measured at 296 K, in a momentum transfer range of 0.1 Å^{-1} < Q < 1.8 Å^{-1}, where Q is the momentum transfer defined by the neutron wavelength (λ) and the scattering angle (2θ) as $Q = (4\pi \sin \theta)/\lambda$. The energy window and resolution were $-40\ \mu eV \leq \hbar\omega \leq 100\ \mu eV$ and $\Delta E = 3.6\ \mu eV$, respectively. The resolution function was determined using a vanadium standard. The counting time was about 3 h for QENS. The QENS data reduction and analyses were performed using software provided by the DNA group of J-PARC MLF.

2.4. Molecular Dynamics (MD) Simulation. Full atomistic MD simulations were carried out on the methanol-dispersed cross-linked phenolic resin model systems. The cross-linked phenolic resin model structures were generated

DOI: 10.1021/acs.macromol.8b00535
Macromolecules 2018, 51, 6334−6343

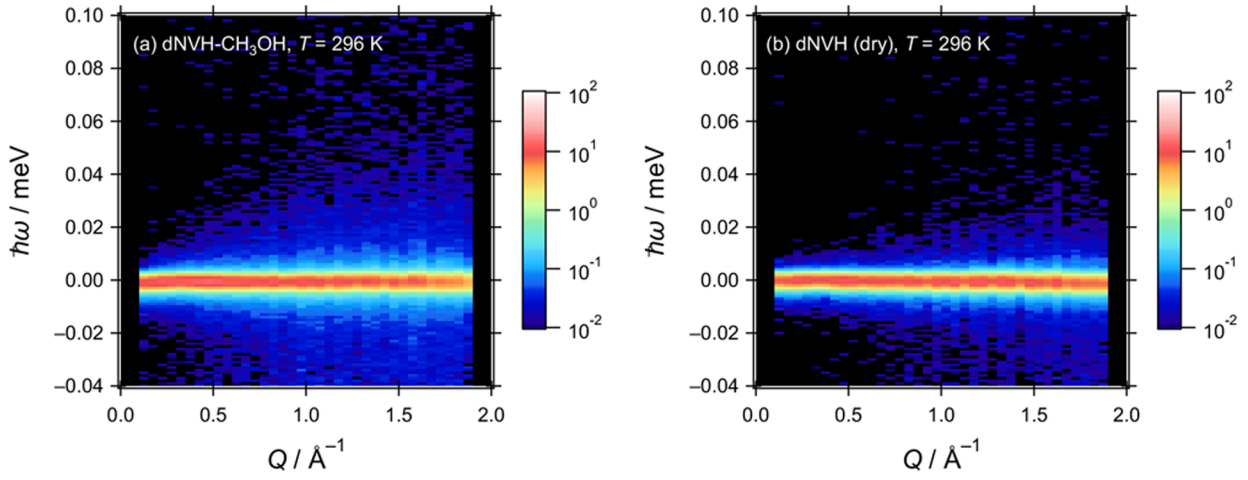

Figure 2. Two-dimensional $S(Q, \omega)$ of (a) dNVH−CH_3OH and (b) dried dNVH.

from phenol molecules via a pseudo-cross-link reaction, as described in our previous research.[32] J-OCTA 1.8 (JSOL Corp, Japan) was used for model construction of phenol and methanol. Partial atomic charges were estimated from RHF/6-31G (d,p) calculation using Gaussian 09 D (Gaussian, Inc., USA) and a restrained electrostatic potential fitting program.[40] The general AMBER force field (GAFF)[41] was applied to the potential function for all molecules. LAMMPS (Sandia National Laboratory, USA)[42] was used for the cross-linking reaction and subsequent MD calculation on the K computer (RIKEN Advanced Institute for Computational Science, Japan). A standard velocity Verlet integrator was used with a time step (Δt) of 0.5 fs in the procedures for all calculations. The Nosé−Hoover thermostat[43,44] and Parrinello−Rahman barostat[45] were used to control the temperature and the pressure, respectively, with a damping parameter of 200 fs for the thermostat and 500 fs for the barostat. Lennard-Jones and Coulombic interactions were computed with a cutoff length of 11 Å and a weighting factor of 0.5 for 1−4 interactions. The particle−particle particle−mesh solver was used to compute long-range Coulombic interactions with the desired relative error in forces within 10^{-5} accuracy.

The model structure for methanol molecules dispersed in a cross-linked phenolic resin was prepared according to the following procedure: First, cross-linked phenolic resins were constructed from 2000 phenol molecules and cross-linker atoms using pseudoreaction algorithms. The details of the cross-linking procedure and features of the resulting structure are described in our previous paper.[32] The degree of cross-linking for the cross-linked phenolic resin was 0.85. This value is nearly identical to the experimental value estimated by solid-state ^{13}C NMR spectroscopy for novolac resins cured with HMTA. Thereafter, 594 molecules of methanol were randomly inserted into the equilibrated phenolic network. The weight fraction of methanol in the resulting structure was approximately 8 wt %, which corresponds to the experimental value. 100 ps of MD was performed with the soft repulsive potential implemented in LAMMPS for nonbonding pairwise interactions instead of using a Lennard-Jones potential. This was selected to break up overlapping atoms and unstable atomic configurations between inserted methanol molecules and the resin. This process ensured that methanol molecules were placed in resin cavities, which are relatively stable structures in terms of energy. Finally, the equilibrated structure was obtained after 2 ns of MD with an *NPT* ensemble under atmospheric pressure and given temperature in the range 220−330 K.

The diffusion coefficient of methanol was estimated from the time dependence of the mean squared displacement (MSD) of methanol molecules using Einstein's relation

$$D = \frac{1}{6}\frac{\mathrm{d}}{\mathrm{d}t}\left\{\frac{1}{N}\sum_{i=1}^{N}[\mathbf{r}_i(t) - \mathbf{r}_i(0)]^2\right\} = \frac{1}{6}\frac{\mathrm{d}}{\mathrm{d}t}\mathrm{MSD}(t) \quad (1)$$

where $\mathbf{r}_i(t)$ represents the coordinates of the center of mass of the ith methanol molecule at time t. In this MD study, at first, the diffusion coefficient of methanol in a bulk liquid state was calculated on the basis of this equation. To confirm the validity of the potential parameters, 500 methanol molecules were placed in an isotropic cubic simulation cell with periodic boundaries for each direction, and *NPT* dynamics was performed to equilibrate the cell size and atomic configuration under atmospheric pressure. Subsequently, 1 ns of MD was carried out to calculate the MSD of methanol molecules using an *NVT* ensemble. D can be obtained from the MSD−t diagram as a gradient. The estimated values of D and the density for bulk methanol at 300 K and at atmospheric pressure were 2.3×10^{-5} cm^2/s and 0.81 g/cm^3, respectively, and are well consistent with the experimental values of $(2.2-2.4) \times 10^{-5}$ cm^2/s and 0.79 g/cm^3.[14,46] The detailed MD result for bulk methanol was described in the Supporting Information.

3. RESULTS AND DISCUSSION

3.1. QENS Experiment. Figure 2 shows the obtained two-dimensional dynamic structure factor $S(Q, \omega)$ of dNVH−CH_3OH and dried dNVH. The dNVH−CH_3OH shows both elastic scattering around $\hbar\omega = 0$ (red band) and quasielastic scattering (blue region). Meanwhile, the dried dNVH shows much less quasielastic broadening than that of dNVH−CH_3OH.

Figure 3 shows the QENS profiles of dNVH−CH_3OH, dNVH−CD_3OD, and dried dNVH normalized by the elastic intensity at $Q = 1.7$ $Å^{-1}$. The difference in scattering intensity between dNVH−CH_3OH and dNVH−CD_3OD indicates the existence of quasielastic broadening from methanol. Furthermore, the larger intensity in dNVH−CD_3OD than that of dried dNVH in the quasielastic region implies the induction of

DOI: 10.1021/acs.macromol.8b00535
Macromolecules 2018, 51, 6334−6343

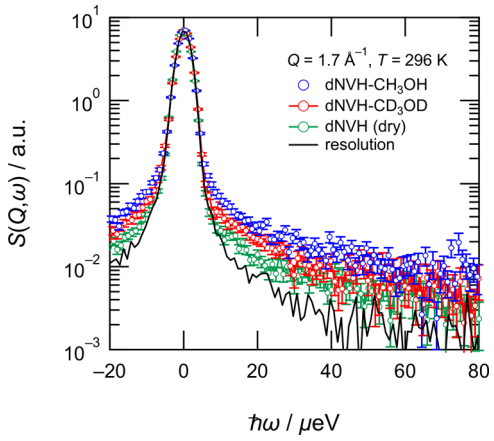

Figure 3. Typical QENS spectra for dNVH−CH_3OH, dNVH−CD_3OD, and dried dNVH at Q = 1.7 Å^{-1}. Spectra are normalized by the elastic intensity.

resin dynamics derived from solvent invasion. Here, this quasielastic scattering is assumed to be from the hydrogen atoms of the cross-linking methylene groups derived from HMTA. As mentioned in our previous study,[32] even in highly cured resin, there are independent clusters of small molecules not belonging to a percolated network. The methylene belonging to such a cluster is plasticized by methanol invasion and exhibits motility.

As previously mentioned, the quasielastic scattering profiles of dNVH−CD_3OD and dNVH in Figure 3 suggest the existence of dynamics in the polymer framework induced by solvent invasion. It is reasonable that the QENS profile of dNVH−CH_3OH is represented by the sum of methanol and dNVH components. Accordingly, eq 2 can be adopted to analyze the scattering profile of dNVH−CH_3OH in this paper

$$S(Q,\omega) = R(Q,\omega) \otimes [A_{el}^{M}(Q)\delta(\omega) + A_{qe}^{M}(Q)L(\Gamma^{M},\omega) + A_{el}^{dNVH}(Q)\delta(\omega) + A_{qe}^{dNVH}(Q)L(\Gamma^{dNVH},\omega)] + \text{bkg.} \quad (2)$$

where $R(Q,\omega)$, $\delta(\omega)$, and $L(\Gamma,\omega)$ are the resolution function of the DNA spectrometer, the delta function, and the Lorentz function, respectively, and bkg. denotes the background. A_{el}^{M}, A_{qe}^{M}, A_{el}^{dNVH}, and A_{qe}^{dNVH} denote the coefficients of each scattering component for elastic and quasielastic scatterings of methanol and elastic scatterings and quasielastic scatterings of dNVH, respectively. Γ^{M} and Γ^{dNVH} represent the HWHM in the Lorentz function of methanol and resin, respectively. Parameters of the dNVH, A_{el}^{dNVH}, A_{qe}^{dNVH}, and Γ^{dNVH} were obtained by the fitting of dNVH−CD_3OD as following eq 3

$$S(Q,\omega) = R(Q,\omega) \otimes [A_{el}^{dNVH}(Q)\delta(\omega) + A_{qe}^{dNVH}(Q)L(\Gamma^{dNVH},\omega)] + \text{bkg.} \quad (3)$$

because the contribution from the CD_3OD was small. The data was well fitted, as shown in Figure 4a. The molar fraction of CH_3OH in the dNVH−CH_3OH system is almost the same as that of CD_3OD in dNVH−CD_3OD. Therefore, Γ^{dNVH}, A_{el}^{dNVH}, and A_{qe}^{dNVH} in eq 2 for dNVH−CH_3OH are regarded to be the same as those for dNVH−CD_3OD. In the subsequent analysis, a parameter fitting was done for A_{el}^{M}, A_{qe}^{M}, and Γ^{M} on the QENS profile of dNVH−CH_3OH using the fixed parameters of A_{el}^{dNVH}, A_{qe}^{dNVH}, and Γ^{dNVH} estimated from the fitting result for dNVH−CH_3OH. The typical fitting result is shown in Figure 4b. The curve fitting was successful using the above-mentioned model.

The Q^2-dependence of Γ^{M} is shown in Figure 5. The Γ of the bulk methanol is also plotted for comparison. The QENS

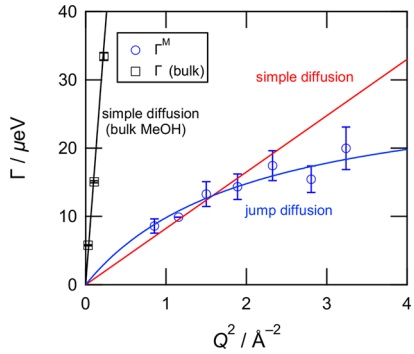

Figure 5. Q^2-dependence of Γ for bulk CH_3OH and Γ^{M} for dNVH−CH_3OH obtained from QENS fitting at T = 296 K. Red and blue lines are fitting results by the simple-diffusion and jump-diffusion models, respectively.

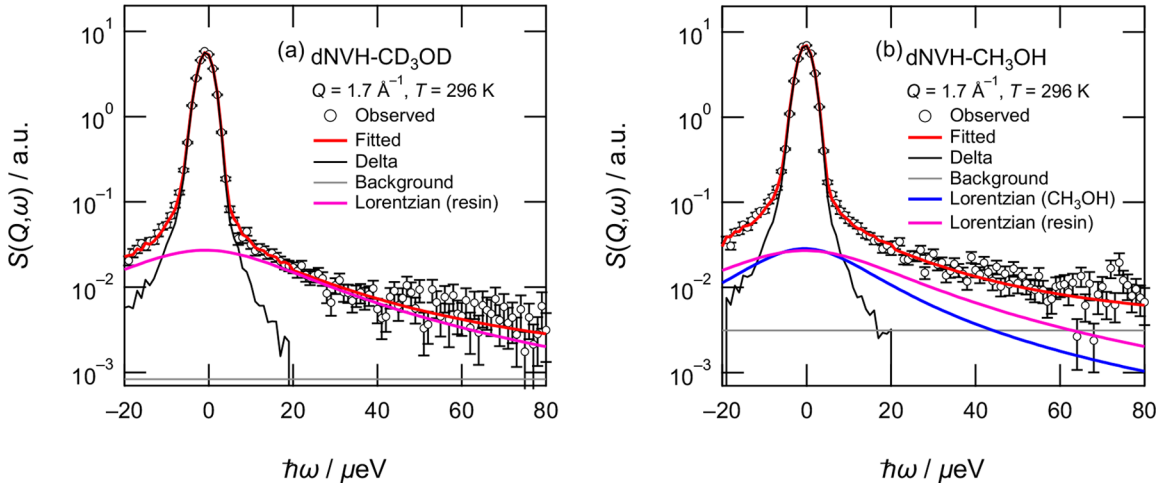

Figure 4. QENS spectra of (a) dNVH−CD_3OD and (b) dNVH−CH_3OH at Q = 1.7 Å^{-1}.

DOI: 10.1021/acs.macromol.8b00535
Macromolecules 2018, 51, 6334−6343

spectra and fitting results for bulk methanol are given in the Supporting Information. In this analysis, the data points of Γ in the range of $Q < 0.8$ Å^{-1} were excluded because the scattering intensity in the low-Q region likely contains an experimental artifact. Q-dependence of Γ usually reflects diffusion-like molecular motions. In the case of continuous diffusion, Γ is expressed as follows

$$\Gamma(Q) = DQ^2 \tag{4}$$

where D is the translational diffusion coefficient.[7,47] The random-jump diffusion model shows the following relationship

$$\Gamma(Q) = \frac{DQ^2}{1 + \tau_0 DQ^2} \tag{5}$$

where τ_0 is the mean residence time. The Q-dependency of Γ for methanol in cured resin well followed a fitting curve of the random-jump diffusion model, though the continuous diffusion model did not match in the high-Q range. The fitting using eq 5 results in $D = 1.6 \times 10^{-6}$ cm^2/s for methanol confined in cured resin, which is 1 order of magnitude smaller than the value in the bulk, $D = 2.3 \times 10^{-5}$ cm^2/s.[13] From the fitting results of $\tau_0 = 14$ ps and $D = 1.6 \times 10^{-6}$ cm^2/s, the mean jump distance $\langle l \rangle = (6D\tau_0)^{1/2}$ in the jump diffusion process can be estimated to be 1.2 Å.

3.2. MD Simulation. Figure 6 shows a 3D image of methanol dispersed in a cross-linked phenolic resin after

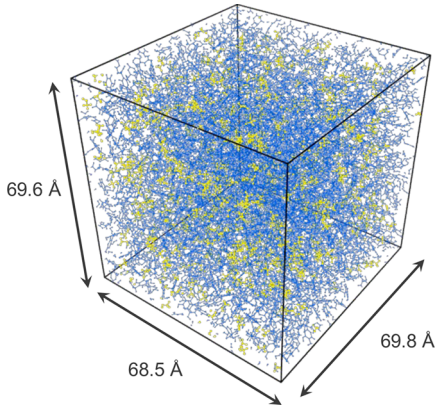

Figure 6. 3D model of methanol molecules (yellow), confined in cured phenolic resins (blue), used in the MD simulation. The number of methanol is 594 in this simulation box.

equilibration at 1 atm and 300 K. The visualization is obtained using the program OVITO.[48] Methanol molecules exist in a vacant space with various sizes. Such a configuration is consistent with the experimental facts of SAXS and SANS, in which voids exist in the network in various sizes ranging from 1 to 1000 nm.[25]

The atomistic configuration of methanol was characterized by hydrogen bonds. Figure 7 shows the radial distribution functions (RDFs) of the O−O pair between the hydroxyl groups of methanol−methanol, methanol−phenol, and phenol−phenol. The existence of peaks at $r = 2.8$ Å for the $g_{OO}(r)$ of phenol−methanol in Figure 7 clearly shows that the hydroxyl groups of methanol molecules in cured resin can form hydrogen bonds to the phenolic network. For the phenolic hydroxyl group, the number of hydrogen bonds was calculated and was summarized in Table 1 according to the definition by Haughney.[49] This result shows approximately 60% of methanol

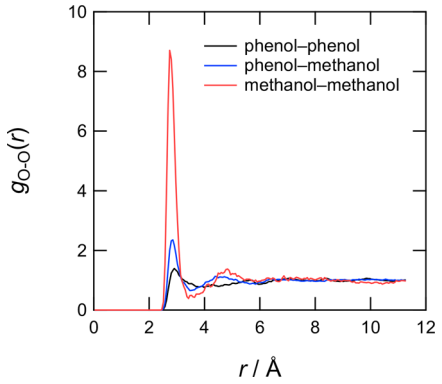

Figure 7. Radial distribution function $g(r)$ of oxygen−oxygen in the MD results for the methanol and phenolic resin system.

Table 1. Number of Free Phenolic Hydroxyl Groups and That Forming a Hydrogen Bond for before (Dried) and after CH_3OH Invasion at 300 K

	dried	after CH_3OH invasion
free	1608	1323
bonded to PhOH	392	332
bonded to CH_3OH		345

molecules form hydrogen bonds to the phenolic hydroxyl groups. The change in the number of phenolic hydroxyl groups forming hydrogen bonds to other phenolic hydroxyl groups is small. This implies that penetrant methanol selectively forms hydrogen bonds with the free hydroxyl groups of phenolic units. These results suggest that methanol molecules in the resin network reside in void spaces near hydroxyl groups of phenolic units and form hydrogen bonds to the phenolic hydroxyl group or other methanol molecule.

This can also be explained by the free space of the resin network using Voronoi tessellation.[32] Voronoi analysis was performed for atoms of the resin network, and the resulting Voronoi volume distribution is shown in Figure 8. Here,

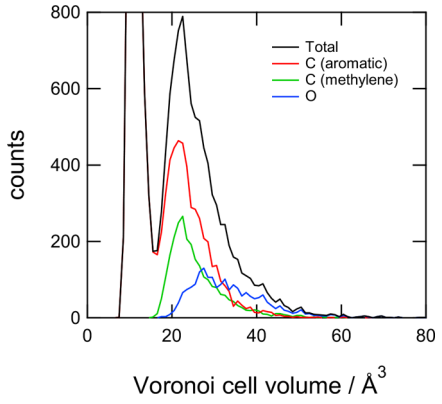

Figure 8. Size distribution of Voronoi volume for carbon and oxygen atoms of the phenolic network.

hydrogen atoms of resins and methanol molecules were excluded for Voronoi tessellation. The strong peaks at Voronoi volumes of 15 and 20 Å^3 in the aromatic carbon atom indicate occupying spaces of substituted and unsubstituted carbons on the benzene ring, respectively. The carbon atom of the methylene linkage and the oxygen atom of the phenolic hydroxyl group have relatively larger Voronoi volumes

DOI: 10.1021/acs.macromol.8b00535
Macromolecules 2018, 51, 6334−6343

compared to aromatic carbon due to smaller topological restriction. The approximate volume of methanol is estimated to be 36.1 Å^3 by using the reported kinetic diameter of 4.1 Å.[50−52] Figure 8 indicates oxygen atoms with a Voronoi volume larger than this value are present at 33%, while there are not many carbon atoms. It is concluded that methanol molecules tend to exist in the void space around the hydroxyl group of phenolic resins.

To understand the local dynamics of methanol in a network from a real-space view, the MSD of the center of mass was calculated for all methanol molecules. The individual MSD of 20 randomly extracted methanol molecules and the averaged MSD curve for all methanol are shown in Figure 9. Note that

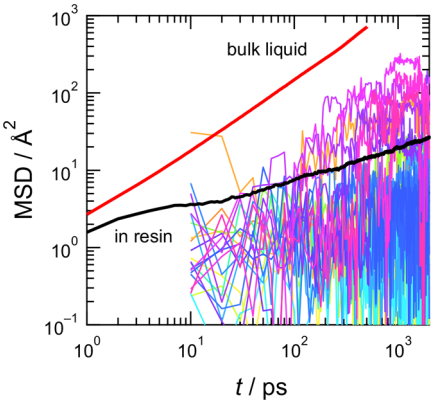

Figure 9. MSD of individual methanol molecules confined in cured phenolic resins (colored lines) and their average (black-bold line) used in the MD simulation. The averaged bulk value is also described for reference (red-bold line).

the calculated MSD in Figure 9 is the instantaneous value at time t. The average curve in the bulk liquid is also given for comparison. This figure clearly shows that the averaged MSD curve in a network (resins) is lower than that in the bulk. The estimated D is 1.6×10^{-7} cm^2/s for the total average in a network and is smaller than those of the bulk liquid (2.3×10^{-5} cm^2/s) and of the above QENS experiment (1.6×10^{-6} cm^2/s). However, the individual MSD curve categorized into several types of methanol; some molecules move greatly, and others do not move at all. To analyze this heterogeneity, the individual D's were calculated for all methanol molecules in the system according to the Einstein relation

$$D_i = \frac{1}{6}\frac{\mathrm{d}}{\mathrm{d}t}[\mathbf{r}_i(t) - \mathbf{r}_i(0)]^2 = \frac{1}{6}\frac{\mathrm{d}}{\mathrm{d}t}\mathrm{MSD}_i(t) \quad (6)$$

where subscript i denotes the ith molecule. The number-average of D_i is the diffusion coefficient originally defined from statistical mechanics. Figure 9 shows the logarithm of the average MSD showed a good linear relationship with the logarithm of time in the range of 50−1000 ps of time. Taking this into account, we regarded 1/6 of the gradient in this range as the diffusion coefficient D. Similarly, D for individual molecules, D_i, is determined as 1/6 of the slope of individual MSD in this range for the sake of convenience.

The distribution of calculated D_i is shown in Figure 10. The histogram shows the existence of D over a wide range, showing inhomogeneous diffusivity of methanol in the network. For further analysis, the methanol molecules are roughly classified into diffusive and nondiffusive modes. Here, we regarded the diffusive one with the larger average diffusion coefficient and

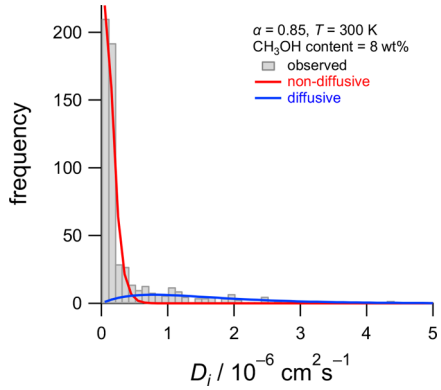

Figure 10. Distribution of D for methanol molecules confined in cured phenolic resins in the MD simulation. The two solid lines are fitting curves by the gamma distribution function.

the nondiffusive smaller one for the fitting results of the D_i distribution with the sum of two gamma distribution functions. The averaged D of diffusive molecules is 1.63×10^{-6} cm^2/s. This result is in good agreement with the QENS experiments, i.e., $D = 1.6 \times 10^{-6}$ cm^2/s. This agreement suggests that our constructed MD model is very reasonable and the existence of confined dynamics for methanol is highly probable. More information about the diffusion behavior of methanol in resin can also be obtained from the time course of the 3D atomic configuration in the MD simulation. Figure 11a shows the trajectory lines of 20 randomly chosen methanol molecules in 2 ns acquired every 10 ps. These molecular trajectories in the MD simulation clearly show that some methanol molecules diffuse by moving a small distance in a limited space, although most methanol molecules are not moving. Such a leaping movement corresponds well to the jump-diffusion model, as suggested from the QENS results. Figure 11b shows an enlarged snapshot of a methanol molecule surrounded by broken lines in Figure 11a. The jump distance between 140 and 150 ps is longer than that of other steps. It corresponds to a leaping step between the void spaces, that corresponds to an instantaneous rapid increase in MSD, as seen in Figure 9. It seems that the dynamics of phenolic resins which is induced by methanol invasion, as suggested by QENS, also contributes to such jumping motion. For reference, the MD results in the case of the resin movement being completely frozen were shown in the Supporting Information.

Figure 12 shows the diffusion coefficient of methanol molecules as a function of reciprocal temperature (T^{-1}) in MD simulation. MD results in bulk liquid were also calculated and presented. For both results, it can be seen that the diffusion coefficient follows the Arrhenius equation, $D = D_0 \exp(-E/k_BT)$, as given by a straight line in the figure, where D_0, E, and k_B are the pre-exponential factor, the activation energy, and the Boltzmann constant, respectively. The values of $D_0 = 5.76 \times 10^{-3}$ (cm^2/s) and $E/k_B = 1.64 \times 10^3$ for bulk liquid well agree with experimental values (4.82×10^{-3} and 1.58×10^3).[49,53] The values for methanol in cured phenolic resins were estimated to be 3.16×10^{-4} and 1.63×10^3, respectively. The agreement of the activation energy suggested that the intermolecular forces on diffusive methanol are equivalent to those on bulk methanol; that is, diffusive methanol forms a hydrogen bond to another methanol or hydroxyl group of phenolic resins. The smaller value of D_0 compared to bulk also

DOI: 10.1021/acs.macromol.8b00535
Macromolecules 2018, 51, 6334−6343

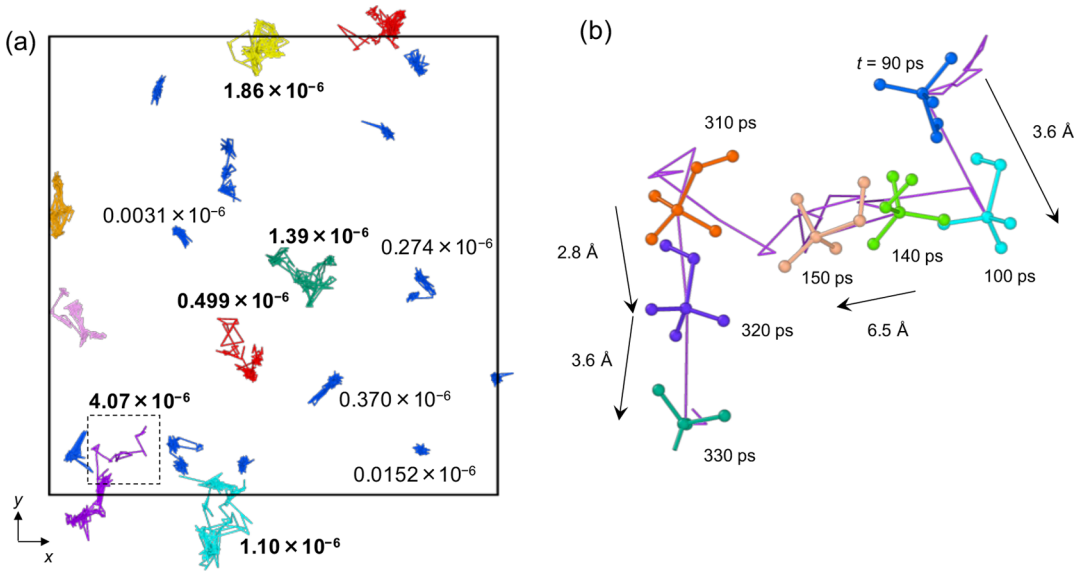

Figure 11. (a) Representative trajectory lines of methanol molecules in 2 ns acquired every 10 ps. The values shown close to the particles indicate D (cm^2/s). Lines of nondiffusive methanol are shown in blue, and lines of diffusive methanol are displayed with different colors. (b) Trajectory of a methanol surrounded by broken lines in part a. Phenolic resin is not displayed to increase visibility for both images.

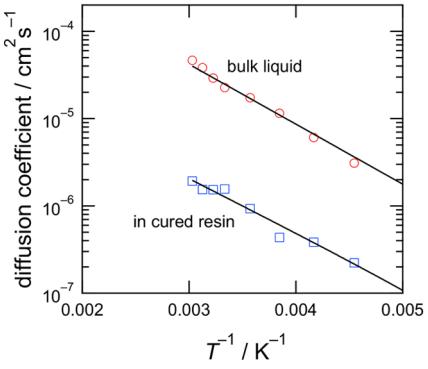

Figure 12. Calculated diffusion coefficients of methanol molecules by MD simulation as a function of reciprocal temperature. The solid line represents fitting by an Arrhenius-type equation.

indicates the existence of steric hindrance of the resin network acting as an interference factor on methanol diffusion.

The above-disclosed results suggest the following solvent penetration model: Penetrating methanol molecules stay in the vacant spaces around the hydroxyl groups of phenolic units for some time and then diffuse by jumping to adjacent void spaces. This process then repeats. In the equilibrium structure, methanol molecules in the network are likely to form hydrogen bonds with the hydroxyl group of phenolic units and other methanol molecules. Hydrogen bonding between penetrating molecules and the polymeric network is recognized as an important factor for solvent swelling in other thermosetting polymers, such as the epoxy resin and water system previously mentioned. This situation is identical to our phenolic resin and methanol system. These results suggest that there are several ways for preventing solvent penetration by small molecules having hydroxyl groups, like water and methanol. One of the solutions would be to reduce the free volume and the fraction of hydroxyl groups in the resin network. Specifically, in a phenolic resin system, changing the molecular weight distribution and the *ortho*/*para* linking ratio in the prepolymer stage before gelation is supposed to be effective, as revealed in our previous MD study.[32] This investigation also showed that QENS analysis is an effective technique for understanding the diffusion behavior of penetrant molecules confined in cross-linked phenolic resins. To prove the versatility of this method for other polymer/solvent systems, further experimental and computational studies will be required.

4. CONCLUSIONS

The diffusion behavior of methanol confined in a cross-linked phenolic resin was investigated by QENS experiments and atomistic MD simulations. In the QENS experiment, a deuterated phenolic resin and methanol (both deuterated and nondeuterated) were used to obtain incoherent scattering functions of methanol because a difference in incoherent scattering cross sections for hydrogen and deuterium was shown. The QENS profiles were well represented as a sum of one elastic and two quasielastic components, indicating the presence of resin dynamics induced by methanol invasion and confined diffusion of methanol molecules. The Q-dependence of the HWHM on methanol revealed that the diffusion coefficient of methanol was 1.6×10^{-6} cm^2/s, which is 1 order of magnitude smaller than the value in the bulk, $D = 2.3 \times 10^{-5}$ cm^2/s, indicating confinement by a polymer network. The MD simulation showed that methanol molecules reside in the vicinity of phenolic hydroxyl groups. Additionally, the presence of diffusive and nondiffusive methanol molecules in highly cross-linked phenolic resins was suggested using mean squared displacement analysis for individual methanol molecules. The MD trajectories showed that some methanol molecules diffuse within a limited space in the resin network by jump-diffusion-like behavior, as suggested by QENS analysis.

This study showed that QENS and MD simulations play important, complementary roles in understanding the diffusion behavior of invading methanol molecules into cross-linked phenolic resins from an atomistic viewpoint. This study also indicated the direction of the molecular design of thermosetting polymers to prevent solvent penetration of methanol, for example, by reducing hydroxyl groups and free volumes by means of adjusting the functional groups and the molecular

DOI: 10.1021/acs.macromol.8b00535
Macromolecules 2018, 51, 6334−6343

weight distribution of prepolymers. We believe these techniques and the findings by this study are applicable to general solvent swelling problems of any thermosetting polymer.

■ ASSOCIATED CONTENT

Supporting Information

The Supporting Information is available free of charge on the ACS Publications website at DOI: 10.1021/acs.macromol.8b00535.

QENS experiment of bulk methanol, MD simulation of bulk methanol, and MD simulation of methanol diffusion in cured resins with fixed dynamics (PDF)

■ AUTHOR INFORMATION

Corresponding Authors

*E-mail: yshudo@sumibe.co.jp.
*E-mail: sibayama@issp.u-tokyo.ac.jp.

ORCID

Atsushi Izumi: 0000-0001-8213-7032
Katsumi Hagita: 0000-0002-6708-7468
Takeshi Yamada: 0000-0001-5508-7092
Mitsuhiro Shibayama: 0000-0002-8683-5070

Notes

The authors declare no competing financial interest.

■ ACKNOWLEDGMENTS

The QENS experiments were executed using the BL02 (DNA) beamline at the Materials and Life Science Experimental Facility (MLF) of J-PARC under Proposal No. 2015A0077 and 2016A0177. This research used computational resources of the K computer provided by the RIKEN Advanced Institute for Computational Science through the HPCI System Research project (Project ID: hp160089). The authors would like to thank Dr. Maiko Kofu of J-PARC center for helpful advice and discussions about the QENS experiments and data analysis.

■ REFERENCES

(1) Gardziella, A.; Pilato, L. A.; Knop, A. *Phenolic Resins: Chemistry, Applications, Standardization, Safety and Ecology*; Springer: Berlin, 2000.
(2) *Phenolic Resins: A Century of Progress*; Pilato, L., Ed.; Springer: Berlin, 2010.
(3) Pascault, J. -P.; Sautereau, H.; Verdu, J.; Williams, R. J. J. *Thermosetting Polymers*; Marcel Dekker: New York, 2002.
(4) Kaplan, M. L. Solvent penetration in cured epoxy networks. *Polym. Eng. Sci.* **1991**, *31* (10), 689−698.
(5) Soles, C. L.; Chang, F. T.; Gidley, D. W.; Yee, A. F. Contributions of the nanovoid structure to the kinetics of moisture transport in epoxy resins. *J. Polym. Sci., Part B: Polym. Phys.* **2000**, *38* (5), 776−791.
(6) Soles, C. L.; Yee, A. F. A discussion of the molecular mechanisms of moisture transport in epoxy resins. *J. Polym. Sci., Part B: Polym. Phys.* **2000**, *38* (5), 792−802.
(7) Bée, M. *Quasielastic Neutron Scattering: Principles and Applications in Solid State Chemistry, Biology and Materials Science*; Adam Hilger: Bristol and Philadelphia, 1988.
(8) *Dynamics of Soft Matter: Neutron Applications*; García Sakai, V., Alba-Simionesco, C., Chen, S. -H., Eds.; Springer: Berlin, 2012.
(9) García Sakai, V.; Arbe, A. Quasielastic neutron scattering in soft matter. *Curr. Opin. Colloid Interface Sci.* **2009**, *14* (6), 381−390.
(10) Mehrer, H. *Diffusion in Solids*; Springer: Berlin, 2009.
(11) Gergidis, L. N.; Theodorou, D. N.; Jobic, H. Dynamics of *n*-butane−methane mixtures in silicalite, using quasielastic neutron scattering and molecular dynamics simulations. *J. Phys. Chem. B* **2000**, *104* (23), 5541−5552.
(12) Colmenero, J.; Brodeck, M.; Arbe, A.; Richter, D. Dynamics of poly(butylene oxide) well above the glass transition. A fully atomistic molecular dynamics simulation study. *Macromolecules* **2013**, *46* (4), 1678−1685.
(13) Bermejo, F. J.; Batallán, F.; Enciso, E.; White, R.; Dianoux, A. J.; Howells, W. S. Diffusional dynamics of hydrogen-bonded liquids: methanol. *J. Phys.: Condens. Matter* **1990**, *2* (5), 1301−1314.
(14) Karger, N.; Vardag, T.; Lüdemann, H. D. Temperature dependence of self-diffusion in compressed monohydric alcohols. *J. Chem. Phys.* **1990**, *93* (5), 3437−3444.
(15) Takahara, S.; Nakano, M.; Kittaka, S.; Kuroda, Y.; Mori, T.; Hamano, H.; Yamaguchi, T. Neutron scattering study on dynamics of water molecules in MCM-41. *J. Phys. Chem. B* **1999**, *103* (28), 5814−5819.
(16) Takahara, S.; Sumiyama, N.; Kittaka, S.; Yamaguchi, T.; Bellissent Funel, M.-C. Neutron scattering on dynamics of water molecules in MCM-41. 2. Determination of translational diffusion coefficient. *J. Phys. Chem. B* **2005**, *109* (22), 11231−11239.
(17) Takahara, S.; Kittaka, S.; Mori, T.; Kuroda, Y.; Takamuku, T.; Yamaguchi, T. Neutron scattering and dielectric studies on dynamics of methanol and ethanol confined in MCM-41. *J. Phys. Chem. C* **2008**, *112* (37), 14385−14393.
(18) Gupta, N. M.; Kumar, D.; Kamble, V. S.; Mitra, S.; Mukhopadhyay, R.; Kartha, V. B. Fourier transform infrared and quasielectron neutron scattering studies on the binding modes of methanol molecules in the confined spaces of HMCM-41 and HZSM-5: Role of pore structure and surface acid sites. *J. Phys. Chem. B* **2006**, *110* (10), 4815−4823.
(19) Mamontov, E.; Burnham, C. J.; Chen, S.-H.; Moravsky, A. P.; Loong, C.-K.; de Souza, N. R.; Kolesnikov, A. I. Dynamics of water confined in single- and double-wall carbon nanotubes. *J. Chem. Phys.* **2006**, *124*, 194703.
(20) Harpham, M. R.; Ladanyi, B. M.; Levinger, N. E.; Herwig, K. W. Water motion in reverse micelles studied by quasielastic neutron scattering and molecular dynamics simulation. *J. Chem. Phys.* **2004**, *121*, 7855.
(21) Rosenberg, H. M. Inelastic neutron scattering in epoxy resins: The phonon-fracton density of states and the specific heat. *Phys. Rev. Lett.* **1985**, *54* (7), 704−706.
(22) Dianoux, A. J.; Page, J. N.; Rosenberg, H. M. Inelastic neutron scattering in the amorphous and the crystalline states: The phonon-fracton density of states. *Phys. Rev. Lett.* **1987**, *58* (9), 886−888.
(23) Arai, M.; Jørgensen, J.-E. Low energy excitation measurement on epoxy resin: The possibility of fracton and phonon-assisted migration. *Phys. Lett. A* **1988**, *133* (1−2), 70−74.
(24) Izumi, A.; Nakao, T.; Shibayama, M. Synthesis and properties of a deuterated phenolic resin. *J. Polym. Sci., Part A: Polym. Chem.* **2011**, *49* (23), 4941−4947.
(25) Izumi, A.; Nakao, T.; Iwase, H.; Shibayama, M. Structural analysis of cured phenolic resins using complementary small-angle neutron and X-ray scattering and scanning electron microscopy. *Soft Matter* **2012**, *8*, 8438−8445.
(26) Allen, M. P.; Tildesley, D. J. *Computer Simulation of Liquids*; Clarendon Press: New York, 1989.
(27) *Computer Simulation of Polymeric Materials: Applications of the OCTA System*; Japan Association for Chemical Innovation, Ed.; Springer: Berlin, 2016.
(28) Yarovsky, I.; Evans, E. Computer simulation of structure and properties of crosslinked polymers: application to epoxy resins. *Polymer* **2002**, *43* (3), 963−969.
(29) Wu, C.; Xu, W. Atomistic simulation study of absorbed water influence on structure and properties of crosslinked epoxy resin. *Polymer* **2007**, *48* (18), 5440−5448.

DOI: 10.1021/acs.macromol.8b00535
Macromolecules 2018, 51, 6334−6343

(30) Li, C.; Strachan, A. Molecular scale simulations on thermoset polymers: A review. *J. Polym. Sci., Part B: Polym. Phys.* **2015**, *53* (2), 103−122.
(31) Izumi, A.; Nakao, T.; Shibayama, M. Atomistic molecular dynamics study of cross-linked phenolic resins. *Soft Matter* **2012**, *8*, 5283−5292.
(32) Shudo, Y.; Izumi, A.; Hagita, K.; Nakao, T.; Shibayama, M. Large-scale molecular dynamics simulation of crosslinked phenolic resins using pseudo-reaction model. *Polymer* **2016**, *103*, 261−276.
(33) Shudo, Y.; Izumi, A.; Hagita, K.; Nakao, T.; Shibayama, M. Structure-mechanical property relationships in crosslinked phenolic resin investigated by molecular dynamics simulation. *Polymer* **2017**, *116*, 506−514.
(34) Izumi, A.; Nakao, T.; Shibayama, M. Gelation and cross-link inhomogeneity of phenolic resins studied by ^{13}C-NMR spectroscopy and small-angle X-ray scattering. *Soft Matter* **2013**, *9*, 4188−4197.
(35) Izumi, A.; Nakao, T.; Shibayama, M. Gelation and cross-link inhomogeneity of phenolic resins studied by small- and wide-angle X-ray scattering and ^{1}H-pulse NMR spectroscopy. *Polymer* **2015**, *59*, 226−233.
(36) Izumi, A.; Shudo, Y.; Nakao, T.; Shibayama, M. Cross-link inhomogeneity in phenolic resins at the initial stage of curing studied by ^{1}H-pulse NMR spectroscopy and complementary SAXS/WAXS and SANS/WANS with a solvent-swelling technique. *Polymer* **2016**, *103*, 152−162.
(37) Shibata, K.; Takahashi, N.; Kawakita, Y.; Matsuura, M.; Yamada, T.; Tominaga, T.; Kambara, W.; Kobayashi, M.; Inamura, Y.; Nakatani, T.; Nakajima, K.; Arai, M. The performance of TOF near backscattering spectrometer DNA in MLF, J-PARC. *JPS Conf. Proc.* **2015**, *8*, 036022.
(38) Seto, H.; Itoh, S.; Yokoo, T.; Endo, H.; Nakajima, K.; Shibata, K.; Kajimoto, R.; Ohira-Kawamura, S.; Nakamura, M.; Kawakita, Y.; Nakagawa, H.; Yamada, T. Inelastic and quasi-elastic spectrometers in J-PARC. *Biochim. Biophys. Acta, Gen. Subj.* **2017**, *1861*, 3651−3660.
(39) Nakajima, K.; et al. Materials and Life Science Experimental Facility (MLF) at the Japan Proton Accelerator Research Complex II: Neutron scattering instruments. *Quantum Beam Sci.* **2017**, *1* (3), 9.
(40) Bayly, C. I.; Cieplak, P.; Cornell, W. D.; Kollman, P. A. A well-behaved electrostatic potential based method using charge restraints for deriving atomic charges: the RESP model. *J. Phys. Chem.* **1993**, *97* (40), 10269−10280.
(41) Wang, J.; Wolf, R. M.; Caldwell, J. W.; Kollman, P. A.; Case, D. A. Development and testing of a general amber force field. *J. Comput. Chem.* **2004**, *25* (9), 1157−1174.
(42) http://lammps.sandia.gov/.
(43) Nosé, S. A unified formulation of the constant temperature molecular dynamics methods. *J. Chem. Phys.* **1984**, *81* (1), 511−519.
(44) Hoover, W. G. Canonical dynamics: equilibrium phase-space distributions. *Phys. Rev. A: At., Mol., Opt. Phys.* **1985**, *31*, 1695−1697.
(45) Parrinello, M.; Rahman, A. Polymorphic transitions in single crystals: a new molecular dynamics method. *J. Appl. Phys.* **1981**, *52* (12), 7182−7190.
(46) Frenkel, M.; Hong, X.; Wilhoit, R. C.; Hall, K. R. In *Thermodynamic Properties of Organic Compounds and Their Mixtures: the Densities of Alcohols* (Landolt−Börnstein - Group IV Physical Chemistry); Hall, K. R., Marsh, K. N., Eds.; Springer-Verlag: Berlin, 2000; Vol. *8G*, pp 11−301.
(47) Egelstaff, P. A. *An Introduction to the Liquid State*; Academic: London, 1967.
(48) Stukowski, A. Visualization and analysis of atomistic simulation data with OVITO−the Open Visualization Tool. *Modell. Simul. Mater. Sci. Eng.* **2010**, *18*, 015012.
(49) Haughney, M.; Ferrario, M.; McDonald, I. R. Molecular-dynamics simulation of liquid methanol. *J. Phys. Chem.* **1987**, *91* (19), 4934−4940.
(50) Van der Bruggen, B.; Schaep, J.; Wilms, D.; Vandecasteele, C. Influence of molecular size, polarity and charge on the retention of organic molecules by nanofiltration. *J. Membr. Sci.* **1999**, *156*, 29−41.
(51) Shah, D.; Kissick, K.; Ghorpade, A.; Hannah, R.; Bhattacharyya, D. Pervaporation of alcohol−water and dimethylformamide−water mixtures using hydrophilic zeolite NaA membranes: mechanisms and experimental results. *J. Membr. Sci.* **2000**, *179*, 185−205.
(52) Ten Elshof, J. E.; Abadal, C. R.; Sekulić, J.; Chowdhury, S. R.; Blank, D. H. A. Transport mechanisms of water and organic solvents through microporous silica in the pervaporation of binary liquids. *Microporous Mesoporous Mater.* **2003**, *65*, 197−208.
(53) Hurle, R. L.; Lawrence, A. W. The effect of isotopic substitution on self-diffusion in methanol under pressure. *Aust. J. Chem.* **1980**, *33*, 1947−1952.

DOI: 10.1021/acs.macromol.8b00535
Macromolecules 2018, 51, 6334−6343